Local Nusselt number evaluation in the case of jet impingement

IOP Conf. Series: Journal of Physics: Conf. Series **1101** (2018) 012018 doi:10.1088/1742-6596/1101/1/012018

Local Nusselt number evaluation in the case of jet impingement

Tomasz Kura[1], Elżbieta Fornalik-Wajs[1], Jan Wajs[2] and Sasa Kenjeres[3]

[1]AGH University of Science and Technology, Department of Fundamental Research in Energy Engineering, al. Mickiewicza 30, 30-059 Krakow, Poland
[2]Gdansk University of Technology, Faculty of Mechanical Engineering, Department of Energy and Industrial Apparatus, ul. Narutowicza 11/12, 80-233 Gdansk, Poland
[3]Delft University of Technology, Faculty of Applied Sciences, Department of Chemical Engineering, van der Maasweg 9, 2629 HZ, Delft, The Netherlands

kura@agh.edu.pl

Abstract. Jet impingement still is one of demanding cases regarding computational fluid dynamics, due to its highly turbulent behaviour, with occurrence of turbulent-laminar transition. Even recently developed methods exhibit some drawbacks – RANS based simulations lack accuracy, LES and DNS based ones require too much computational time. Hybrid methods also exist, but their development and validation is in progress. Nevertheless, CFD application can play major role in the investigation of jet impingement phenomena. While the flat surface impingement is widely discussed in the literature, there is lack of data regarding non-flat surfaces – the ones that might exist for example in the heat exchangers. In the following paper, the numerical simulation of both flat and non-flat surfaces single jet impingement is presented, with the aim of precise description of the turbulence models impact on the thermal and hydrodynamic results. Choice of turbulence model is crucial for sufficient calculation outcome. Only the complex analyses, shown in the article, including the turbulence and momentum budgets comparison between particular models, can reveal significant and meaningful differences.

1. Introduction

Jet impingement phenomena is applied for the heat transfer enhancement for many years – for example in turbine blade cooling or metallurgy. Wajs et al. [1-3] proposed and verified another implementation of this method. They presented a prototype of cylindrical heat exchanger, in which numerous orifices generate turbulent jets. In contact with the heat exchanging surface they interfere with boundary layer, causing significantly higher heat rates transferred between the cold and hot fluid sides. The experimental results were very promising, but only general parameters, such as overall heat transfer coefficient, total pressure losses etc., were available. The reason of such positive effect on performance, regarding non-flat surfaces, was an interesting problem to be investigated, especially in the light of future optimization. This issue is poorly described in the literature and it demonstrates lack of universal correlations describing heat transfer phenomena. Therefore the numerical methods, especially their ability to perform multiscale analyses, can lead to better understanding of phenomena occurring in the near-wall zones of heat exchangers. Because of relatively short computation time the RANS methods were used as the first ones. They can be important for the analyses of the single jet, but crucial when the jet arrays will be considered with additional crossflow – the conditions which

exist in the abovementioned heat exchanger. The selection of particular RANS model is necessary for the reliable results. Unfortunately, according to Zuckerman [4], the unresolved issue of heat transfer prediction is common for almost all available RANS models. The one recognized as presenting the best performance is Durbin's v^2-f [5]. Its theoretical superior performance was reported for example by Behnia [6, 7]. In the following paper, this model was validated for single jet impingement on flat and non-flat surfaces. It is important from the future, more detailed analyses of real heat exchangers, point of view. Its more recent, modified version, ζ-f by Hanjalic et al. [8], is also taken into account. Calculations were conducted with utilization of the OpenFOAM software, in which the first model is implemented by default, while the second one was implemented by the Authors. The ultimate goal is to choose the RANS model that would be used in the future for the custom hybrid RANS/LES simulations – in Authors opinion the best one to investigate such complex devices.

2. Mathematical model, geometry and numerical procedure

The analyses required consideration of mass (1), momentum (2) and energy (3) conservation laws [9]. Simulations, performed with open-source OpenFOAM software, were steady state and incompressible, performed using 2D geometries. For the single jets impingement, steady state is possible to be used, due to chosen boundary conditions. Reynolds averaging approach was utilized. Classic SIMPLE method was included, and all numerical schemes were of second-order types. The air was used as the working medium.

$$\frac{\partial \overline{u_i}}{\partial x_i} = 0, \tag{1}$$

$$\rho \frac{\partial}{\partial x_j}\left(\overline{u_j}\,\overline{u_i}\right) = -\frac{\partial \overline{p}}{\partial x_j} + \frac{\partial}{\partial x_j}\left(2\mu S_{ij} - \rho \overline{u_i' u_j'}\right), \tag{2}$$

$$\frac{\partial}{\partial x_j}\left(\overline{u_j}\Theta\right) = \frac{\partial}{\partial x_j}\left(\alpha \frac{\partial \Theta}{\partial x_j} - \overline{u_j \theta}\right), \tag{3}$$

where $u_{i,j}$ are the velocity components, m/s; ρ is the density, kg/m^3; p is the pressure, Pa; μ is the dynamic viscosity, Pa·s; S_{ij} is the strain rate tensor, 1/s; $\overline{u_i' u_j'}$ is the Reynolds stress term, m^2/s^2; Θ is the mean temperature, K; α is the thermal diffusivity, m^2/s and $\overline{u_j \theta}$ is the turbulent heat flux. The symbol "¯" represents averaged quantity.

In figure 1, the geometries of flat and non-flat cases are shown. Presented dimensions correspond with the ones included in the ERCOFTAC association database [10] – they assure reliable validation of chosen numerical approach. As it can be seen, axisymmetric geometries were investigated. In the non-flat type cases, dimension H is the same as in the flat case. One additional parameter – curvature radius R, was introduced. Its value, the same for convex and concave types, was chosen on the basis of Authors' previous publication [11]. Moreover, it corresponds with the radius from the heat exchanger [1-3].

In table 1, list of boundary conditions and their values is presented. Flow at the orifice exit was fully developed, which was achieved with the boundary mapping technique. Conditions were chosen to correspond with the ERCOFTAC [10] reference data. Apart from validation with reference case, the computational space division was validated with mesh independence tests.

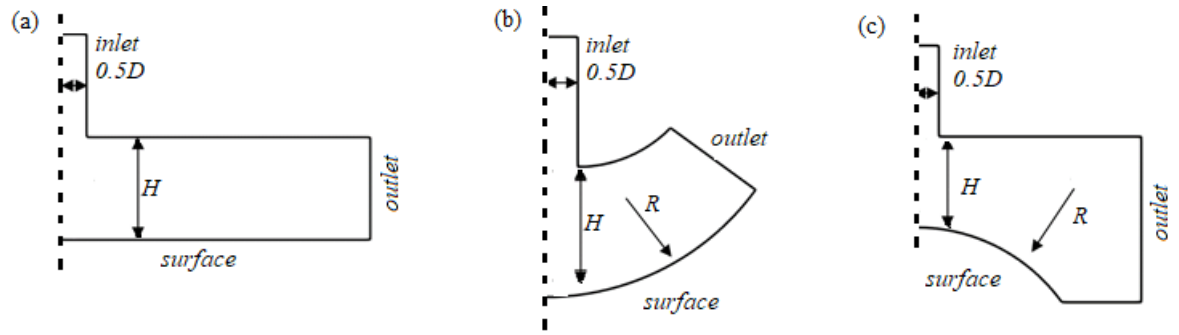

Figure 1. Types of analyzed geometries, (a) flat, (b) concave and (c) convex.

Table 1. Boundary conditions

Bulk Reynolds number, orifice exit	Temperature, orifice exit, K	Heat flux density at the surface, W/m^2	*H/D*	*R/D*
23000	293	1000	2	4

3. Results

Comparison of obtained data was performed in the basis of on the local velocity profiles, local Nusselt number values, local turbulence and momentum budgets. Therefore it was important to establish the method for flat and non-flat geometries comparison. Figure 2 presents, how the reference points were determined. For analyzed cases, the differences of the chord length and corresponding segment connecting those points and stagnation points were negligible – as a results, the non-dimensional distance *x/D* was used as sufficient and reliable parameter.

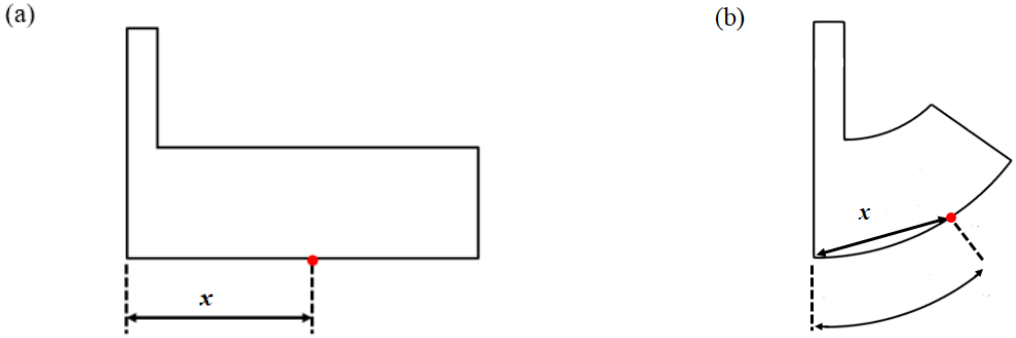

Figure 2. Determination of the reference point, (a) flat and (b) non-flat cases.

3.1. Velocity profiles

At first, the local velocity profiles normal to the heated surface, obtained with v^2-f and ζ-f models for the flat geometry were compared with the reference data, to check their accuracy. Results are presented in figure 3. As it can be seen, the shape is very similar, however slightly better agreement with the experimental data for the ζ-f model could be found.

Since the ζ-f represented good matching with the experimental data, it was selected to obtain the local velocity profiles for non-flat surfaces. Comparison of the results with flat case is shown in figure 4. The most visible differences could be observed in the region close to the stagnation point.

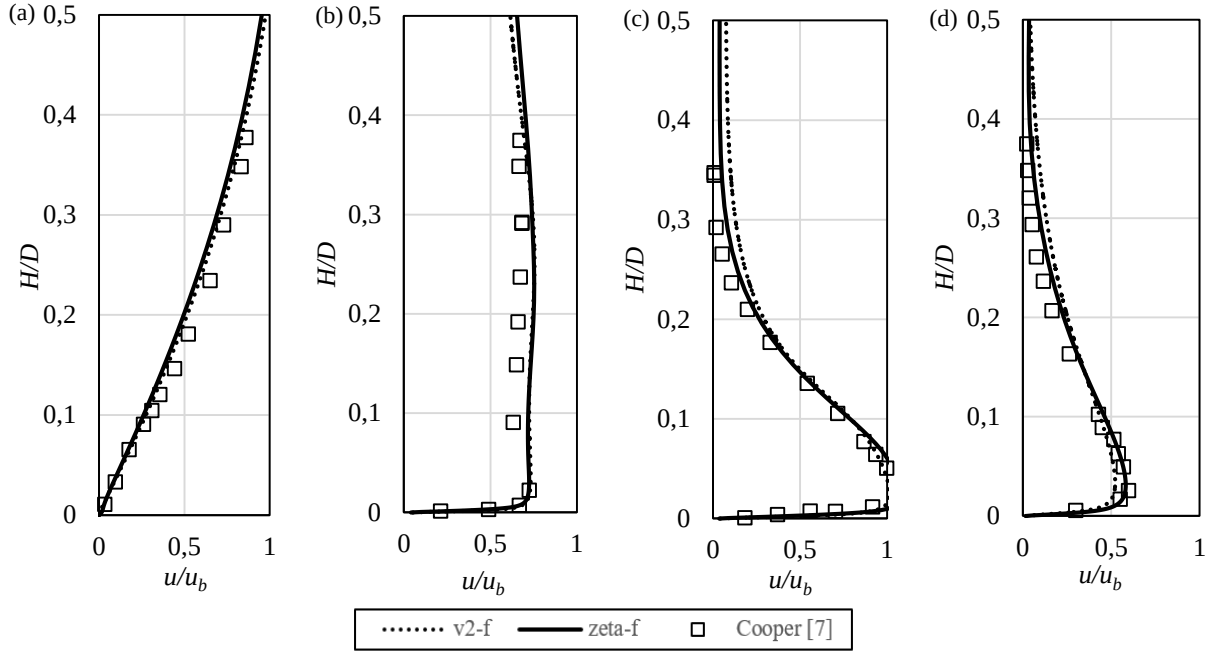

Figure 3. Local velocity profiles at selected radial locations, normalized by bulk velocity in the orifice exit u_b, (a) x/D = 0, (b) x/D = 0.5, (c) x/D = 1, (d) x/D = 2.5. Flat surface, v^2-f vs ζ-f.

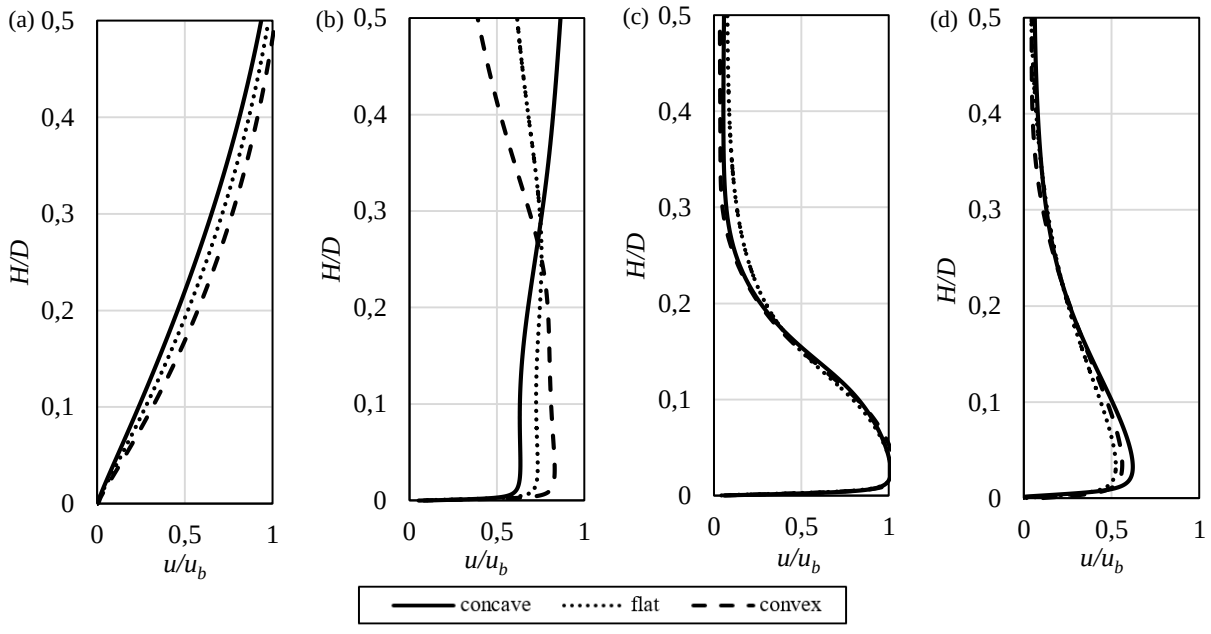

Figure 4. Local velocity profiles at selected radial locations, normalized by bulk velocity in the orifice exit u_b, (a) x/D = 0, (b) x/D = 0.5, (c) x/D = 1, (d) x/D = 2.5. All surface types, ζ-f model.

3.2. Local Nusselt number

Another comparison was done for the local Nusselt number distribution along the heated surface, defined by equation (4):

$$\mathrm{Nu} = \frac{h_{ef} D}{\lambda}, \tag{4}$$

h_{ef} is the effective heat transfer coefficient, W/(K·m^2), obtained locally with the use of the software and λ is the thermal conductivity, W/(K·m). This parameters is crucial for the analysis of heat exchangers.

In figure 5(a) the local Nusselt number values, obtained with both considered models, are presented and compared with the experimental and numerical data from ERCOFRACT database. Surprisingly, results by Behnia [6, 7], who used v^2-f model, are in poor agreement with the ones obtained by Authors using the same model in the stagnation zone. On the other hand the results obtained with ζ-f model, very adequate in the stagnation zone, are slightly over-predicting the Nusselt number values far from it. However the most important feature of the phenomena – secondary peak, demonstrated by the experimental results and located close to the the x/D value equal to 2, is successfully predicted by ζ-f model. The reason of such noticeable discrepancy in both v^2-f results comes from the fact, that the model commonly implemented in CFD software is not the original one [12]. Changes applied by Lien and Kalitzin [13] made it more robust, but at the same time less precise. Hanjalic [8], who also modified the original v^2-f, proposed different approach, which led to better accuracy, as presented here. In figure 5(b), comparison of the local Nusselt number parameter, for various surface types, is presented. The differences between the results are not significant at the stagnation zone and near it, but increase at longer distance. Importance of this discrepancy may increase when instead of single jet, whole array of impinging jets would be analyzed.

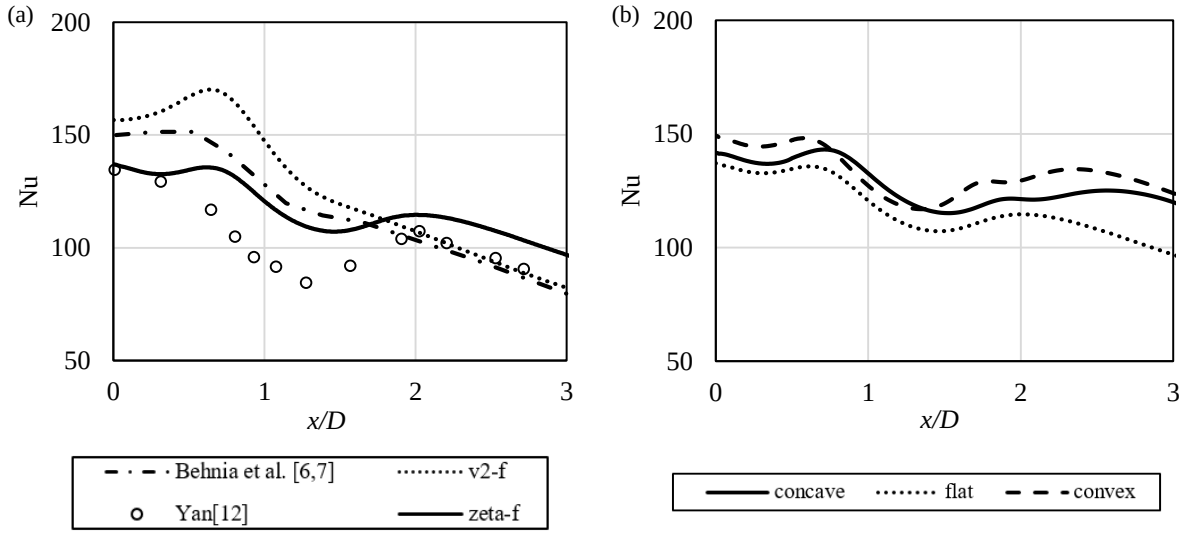

Figure 5. Local Nusselt number distribution along the heated surface, (a) comparison of the turbulence models results, flat surface and (b) comparison between analyzed surface types.

3.3. Turbulence budgets

While the velocity profiles do not differ much between both investigated turbulence models, the uncertainties coming from the local Nusselt number results require identification of their source. One possible way is to check the turbulence kinetic energy (k) budget, as the turbulent character of the flow is expected to play major role in the heat transfer intensification in the heat exchanger [1-3]. The terms of kinetic energy of turbulence were determined in accordance with their representation in [9]. In figure 6, all the terms representing particular parts of the turbulence kinetic energy budget are shown. For this particular analysis, their values were obtained on the curve equally distant from the heated surface. Distance between them was chosen to correspond with the distance between the maximum value of turbulence kinetic energy and the surface. As it can be concluded from the results shown in figure 6, the overall tendency is the same for all types of surfaces, the only differences refer to the maximal values and their positon x/D. However, this statement is checked only for analyses of non-flat surfaces, in which R/D ratio was equal to 4. Its universality have to be verified for more configurations.

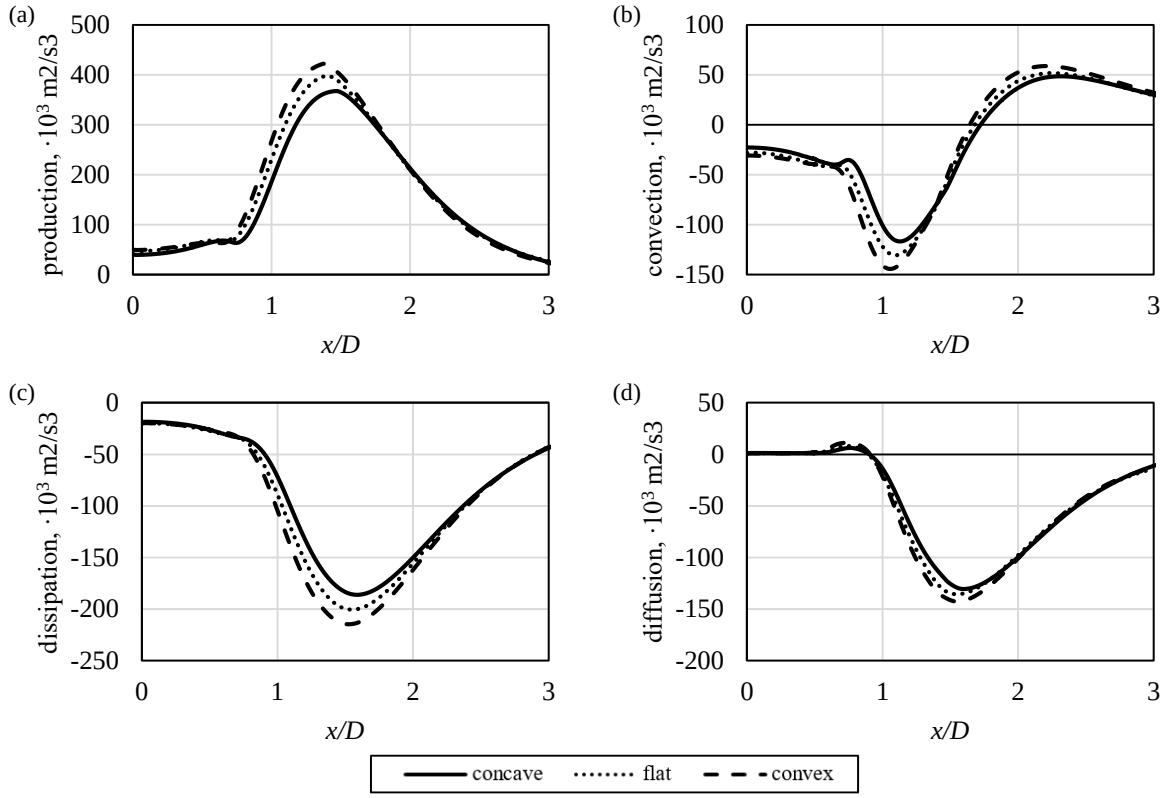

Figure 6. Kinetic energy of turbulence budget, (a) production, (b) convection, (c) dissipation and (d) diffusion. *ζ-f* model.

It is important to note, that in figure 6, the results obtained with Hanjalic model are presented. In figure 7(a), the production term for all simulated geometries is shown, obtained when using Lien and Kalitzin v^2-*f* model. This time, significant differences between each case exist in the stagnation zone. Noticeable peak of production term in the stagnation zone, not present when *ζ-f* model was used, is the main reason of heat transfer over-prediction, mentioned in the section 3.2. It has to be compensated in the stagnation zone by other terms, here represented for example by the higher values of dissipation term, shown in figure 7(b). In general, particular curves are characterized by higher values for v^2-*f* model.

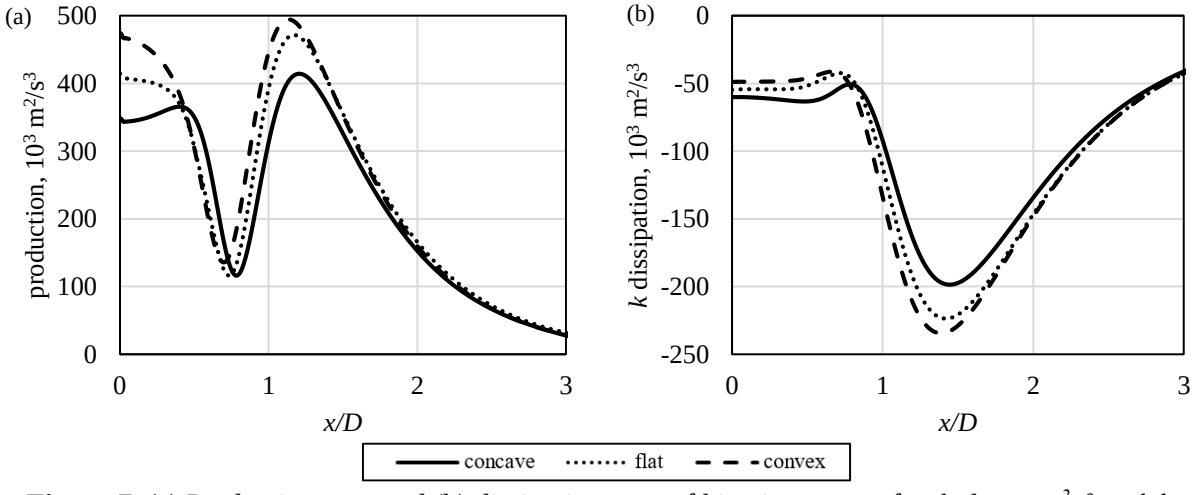

Figure 7. (a) Production term and (b) dissipation term of kinetic energy of turbulence, v^2-*f* model.

3.4. Momentum budgets

The differences in the local Nusselt number values presented in figure 5(a) and the questions raised by them led also to comparison of particular terms of the momentum budget. In figures 8 and 9, the results calculated with two analyzed models, at the location of *x/D* equal to 0.5 and 2 are presented. The first location represents the place, where stagnation zone starts to vanish, the second location represents the place, where secondary Nusselt peak occurred.

One noticeable feature of v^2-*f* model is the significantly higher diffusion of momentum near the wall, visible in figures 8(a) and 9(a) – probably it plays a role in turbulence limitation near the wall, which is the main issue with v^2-*f*, as described in section 3.3.

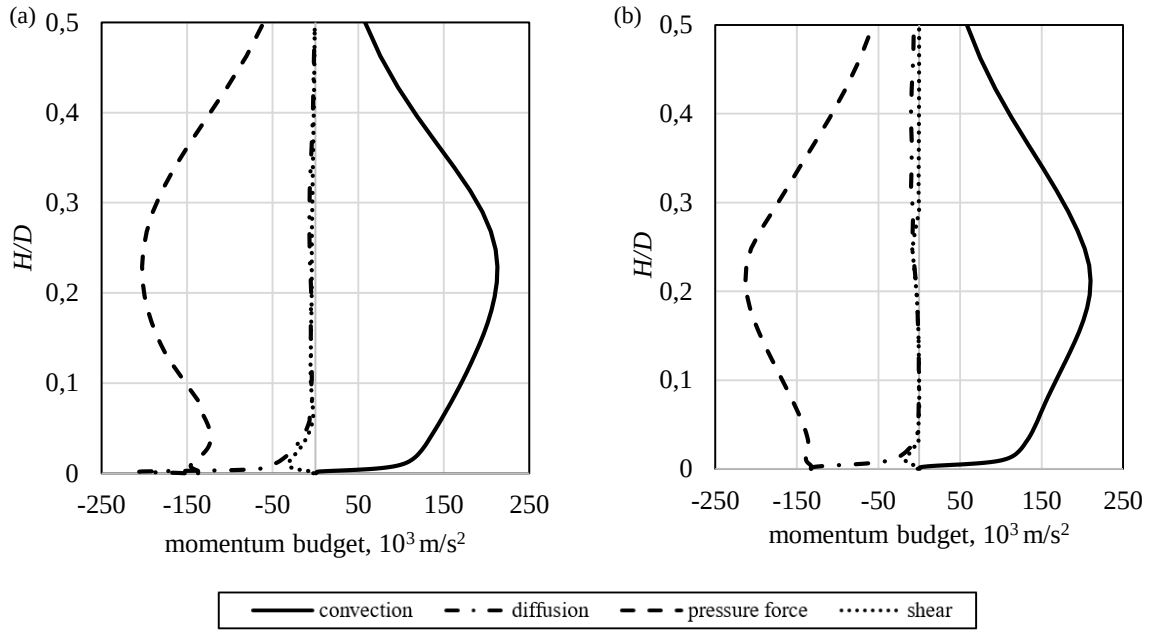

Figure 8. Momentum budget terms, *x/D* = 0.5. (a) v^2-*f* model and (b) ζ-*f* model.

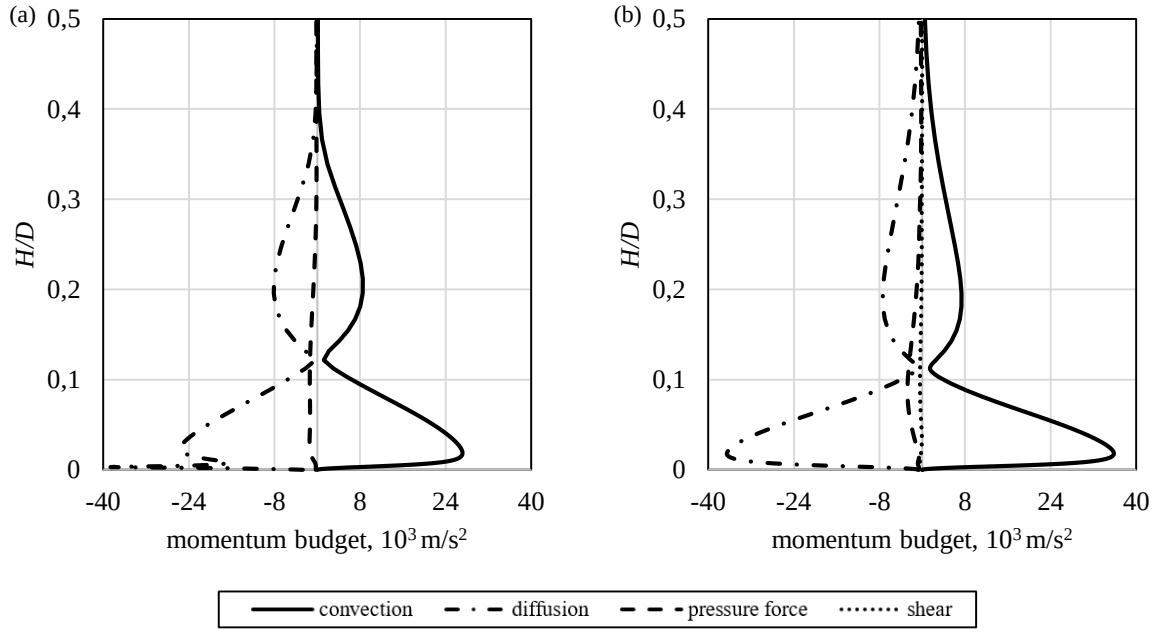

Figure 9. Momentum budget terms, *x/D* = 2. (a) v^2-*f* model and (b) ζ-*f* model.

4. Summary

This paper discussed the performance of two RANS turbulence models, v^2-f and ζ-f, implemented in the OpenFOAM software, in the case of flat and non-flat surfaces jet impingement. The main goal was to determine the model that can be further used in preparation of hybrid RANS/LES model to perform complex analysis of phenomena occurring in the heat exchanger [1-3].

Both models were selected in the basis of literature overview and their ability to simulate cases of jet impingement. However, as revealed in the following work, both models exhibit some disadvantages, that need to be overcome before performing more advanced analysis. It can be stated, that Hanjalic ζ-f [8] model is more suitable for the future purposes. It is able to better predict the heat transfer rates, moreover it does not over-predicts turbulence generation in the stagnation regions. In addition, it turns out to be numerically stable. It is worth to mention that to make the presented results more reliable, also more recent, 2012 Billard and Laurence [12] RANS model, in opinion of its creators the most accurate 4 equations v^2-f based model, was included in the research. It turned out however to be very unstable with higher order numerical schemes, also obtained heat transfer rates were not satisfactory. The results therefore were not included in this paper.

To sum up, only very detailed analysis of particular turbulence model can explain the reasons of its better or worse representation of real problem. With understanding of particular terms and variables, its tuning can be performed, which can lead to improvement of the simulation results.

5. References

[1] Wajs J Mikielewicz D Fornalik-Wajs E 2013 *Cylindrical jet heat exchanger dedicated to heat recovery, especially from low temperature waste sources* (Patent PL224494, in Polish)
[2] Wajs J Mikielewicz D Fornalik-Wajs E Bajor M 2015 *Arch. of Thermodynamic* **36** 48-63
[3] Wajs J Mikielewicz D Fornalik-Wajs E Bajor M 2018 *Heat Tr. Eng.* doi:10.1080/01457632.2018.1442369
[4] Zuckerman N Lior N 2005 *J. Heat Transfer* **127** 544-552
[5] Durbin P A 1995 *AIAA Journal* **33** 659-664
[6] Behnia M Parneix S Durbin P A 1998 *Int. J Heat Mass Transfer* **41** 1845-1855
[7] Behnia M Parneix S Shabany Y Durbin P A 1999 *Int. J. Heat and Fluid Flow* **20** 1-9
[8] Hanjalic K Popovac M Hadziabdic M 2004 *Int. J. Heat Fluid Flow* **25** 1047–1051
[9] Holzmann T *Mathematics, Numerics, Derivations and OpenFOAM* (online book)
[10] Cooper D Jackson D C Launder B E Liao G X 1993 *Int. J. Heat Mass Transfer* **36** 2675-2684
[11] Kura T Fornalik-Wajs E Wajs J 2018 *Arch. of Thermodynamics* **39** 147-166
[12] Billard F Laurence D 2012 *Int. J. Heat Fluid Flow* **33** 45-58
[13] Lien F S Kalitzin G 2001 *Int. J. Heat Fluid Flow* **22** 53-61

Acknowledgments

The present work was supported by the Polish Ministry of Science and Higher Education and by the PLGrid Infrastructure.